J Mater Sci (2016) 51:5857–5871

Synergistic effect of expandable graphite and intumescent flame retardants on the flame retardancy and thermal stability of polypropylene

Zaihang Zheng[1,2,*], Yan Liu[2], Long Zhang[1], and Hongyan Wang[3]

[1] School of Chemical Engineering, Changchun University of Technology, Changchun 130012, People's Republic of China
[2] Key Laboratory of Bionic Engineering (Ministry of Education), Jilin University, Changchun 130022, People's Republic of China
[3] College of Chemistry, Jilin University, Changchun 130012, People's Republic of China

Received: 14 November 2015
Accepted: 8 March 2016
Published online: 15 March 2016

ABSTRACT

In this article, the investigation mainly focuses on the synergistic effect of expandable graphite (EG) and intumescent flame retardants in improving the flame retardancy of polypropylene (PP). The ratio of melamine polyphosphate (MPP) and dipentaerythritol (DPER) has been studied by limiting oxygen index (LOI) and vertical burning test (UL-94) tests. The results demonstrate that the optimal ratio of MPP and DPER in flame-retarding PP was 3/1. Except that, the incorporation of EG into the PP/MPP/DPER system can greatly improve the flame-retardant properties of PP materials. When the content of EG is 10 wt%, LOI value of PP composites reaches 33.2 % and obtains V-0 rating in UL-94 tests. Furthermore, Fourier transform infrared spectra (FTIR) indicate that the main char-formation process of this system occurs at 350–400 °C. And char residue for PP composites after combustion was systematically analyzed by FTIR and X-ray photoelectron spectroscopy spectra. Based on these facts, a potential condensed flame-retardant mechanism was primarily proposed.

Introduction

Due to the versatility, high performance-to-cost ratio, easy processing, and excellent mechanical properties, polypropylene (PP) materials possess quite wide actual application, such as containers, automobiles, non-woven fabrics, construction, coverings, wires and cables, electronic and electric industry [1–3]. Unfortunately, the inherent flammability of PP materials when exposed to fire severely restricts the further application in more fields. Thus, the improvement in flame-retardant properties of PP materials has become an urgent and attractive topic all over the world.

Recently, halogen-free intumescent flame retardants (IFR) become the major trend in flame-retarding polymers because of low smoke release, low toxicity, and anti-dripping properties [4–6]. In this condition, the research on halogen-free IFR has

Address correspondence to E-mail: zhengzaihang@ccut.edu.cn

DOI 10.1007/s10853-016-9887-6

attracted more and more attention in the fields of flame retardants. Traditionally, halogen-free IFR system is mainly composed of three elementary ingredients: acid source, charring agent, and blowing agent. Until now, the most typical halogen-free IFR system is a mixture of ammonium polyphosphate (APP), pentaerythritol (PER), and melamine (MEL). Bourbigot and his co-workers have done extensive experiments and research on the intumescent flame-retardant system in flame-retarding polyolefins [7, 8], and reviewed the recent development of the IFR systems in great detail [7]. Camino et al. also have systematically studied the intumescent behavior and flame retardancy of APP/PER systems with pentaerythritol diphosphate (PEDP) as a model compound [9–14]. The main mechanism of an intumescent flame-retardant system can be ascribed that when the materials are heated above a critical temperature, the formation of dense layer on the surface and foam-like structure inside the materials via the chemical reaction among these additives during thermal degradation of polymers. Here, compact char layer is produced by the esterification and cross-linking interaction between acid source and charring agent, which can swell and expand under the inert gases release from the thermal decomposition of blowing agent. Thus, these additives act as a significant role in forming a carbonaceous char, which can function as a physical barrier to limit the heat and mass transfer and diffusion of inflammable gases between gas and condensed phase. Expandable graphite (EG) is another type of intumescent flame retardant, which is an inherent graphite form with intercalation structure. It is a layered crystal consisting of sheets of carbon atoms tightly bound to each other by conjugated and delocalized π–π bonds [15]. In the preparation process, the sulfuric acid and nitric acid are inserted into the gaps between the carbon layers. When exposed to heat, EG promotely expands to generate a voluminous insulative worm-like layer and provides fire-retardant performance to polymers. Nowadays, EG is widely employed as a blowing agent and smoke suppressor. However, the rapid reaction of EG during thermal flow leads to the non-directional expansion that can weaken the dense and compact char layer combustion of polymer composites. That is the so-called "popcorn effect" [16]. However, few papers report the combination of IFR and EG in improving the flame-retardant properties of polymer materials that are by the common reinforcement effect of two materials in enhancing the char layer structure.

In this article, the aim is to discuss the synergistic effect between IFR and EG in improving the quality of the char layer for PP composites during combustion. The IFR system was composed of melamine polyphosphate (MPP) and dipentaerythritol (DPER) that act as an acid source and char-forming agent, respectively. The optimum ratio of MPP and DPER and the effect of EG on the IFR system were systematically investigated by thermogravimetric analysis (TGA) and flame retardancy tests. FTIR spectra of char residue for IFR/EG in different temperatures propose the formation process of char layer occurs at 350–400 °C. Except that, limiting oxygen index (LOI) and vertical burning (UL-94) tests indicate that the highest LOI value of PP/IFR/EG is 33.2 % and it can obtain a V-0 rating. Moreover, the residue of PP composites after combustion analyzed by optical photos, FTIR spectra, and XPS spectra can deduce the flame-retardant mechanism of IFR/EG in PP matrix, which experiences a typical condensed flame-retardant procedure.

Experimental

Materials

PP (melt flow index, 2.5 g/10 min) was provided by Yangzi Petroleum Chemical Company. Dipentaerythritol (DPER) was obtained from Sinopharm Chemical Reagent Co., Ltd. Melamine polyphosphate (MPP) was purchased from Qingdao Haida Chemical Co., Ltd. Before using, DPER and MPP were dried at 80 °C for 12 h. Expandable graphite (EG, expansion rate 100–150 mL/g) was purchased from Qingdao Tianhe Graphite Co., Ltd.

Preparation of flame-retarding PP composites

PP and flame retardants were melt-mixed in a twin-roller mill (manufactured by Wuhan Ruiming Plastic Machinery Factory, SJSZ-10) at a temperature about 180–190 °C for 15 min. The roller speed was 30 rpm. After mixing, the samples were hot-pressed at about 190 °C under 10 MPa for 10 min into sheets of suitable size for measurements. The detailed formulation is given in Table 1.

Table 1 The results of LOI and UL-94 tests for PP composites

Sample code	PP	MPP	DPER	EG	LOI	UL-94			
	wt%	wt%	wt%	wt%	%	3.2 mm	Dripping	1.6 mm	Dripping
PP	100	–	–	–	17.0	NR	Yes	NR	Yes
PP/MPP	100	30	–	–	24.5	NR	Yes	NR	Yes
PP/DPER	100	–	30	–	21.0	NR	Yes	NR	Yes
PP/EG	100	–	–	30	25.5	NR	Yes	NR	Yes
PP/MPP/DPER 1/3	100	7.5	22.5	–	26.2	V-2	Yes	NR	Yes
PP/MPP/DPER 1/2	100	10.0	20.0	–	26.9	V-1	No	NR	Yes
PP/MPP/DPER 1/1	100	15.0	15.0	–	27.6	V-1	No	V-2	Yes
PP/MPP/DPER 2/1	100	20.0	10.0	–	28.2	V-0	No	V-2	Yes
PP/MPP/DPER 3/1	100	22.5	7.5	–	28.7	V-0	No	V-1	No
PP/MPP/DPER 4/1	100	24.0	6.0	–	27.8	V-1	No	V-1	No
PP/IFR/EG 2.5	100	20.6	6.9	2.5	29.3	V-0	No	V-1	No
PP/IFR/EG 5.0	100	18.7	6.3	5.0	30.1	V-0	No	V-1	No
PP/IFR/EG 7.5	100	16.9	5.6	7.5	31.7	V-0	No	V-1	No
PP/IFR/EG 10.0	100	15.0	5.0	10.0	33.2	V-0	No	V-0	No
PP/IFR/EG 12.5	100	13.1	4.4	12.5	32.5	V-0	No	V-1	No
PP/IFR/EG 15.0	100	11.2	3.8	15.0	32.1	V-1	No	V-1	No

Measurements and characterization

Fourier transform infrared spectra (FTIR)

The infrared spectra of the samples were recorded with an FTIR SHIMADZU spectrometer at a resolution of 2 cm^{-1}. FTIR spectra of the samples were obtained between 4000 and 400 cm^{-1} on a KBr powder with an FTIR spectrometer.

Thermogravimetric analysis (TGA)

All of samples were dried overnight before measurement. The TGA curves were recorded on a Pyris Diamond TG/DTA (Perkin Elmer, USA) under 50 ml/min nitrogen flow ratio from 50 to 850 °C at a heating rate of 10 °C/min. The weights of samples were 5–10 mg. The calculated TGA and DTG curves were summed up by the TGA curves of the mixture ingredients weighted by their contents [17].

$$W_{\mathrm{cal}}(T) = \sum_{i=1}^{n} \mathrm{xi}Wi(T),$$

where x_i is the content of compound i and W_i is TGA curve of compound i.

X-ray photoelectron spectroscopy (XPS) spectra

The XPS spectra were recorded with a VG ESCALAB MK II spectrometer using Al ka excitation radiation (hν = 1253.6 eV).

Limiting oxygen index (LOI)

The LOI tests were carried out by using an XZT-100A oxygen index test instrument (Chengde Jiande test instrument Co., Ltd., China) based on the standard LOI test, ASTM D 2863-97. The dimensions of specimens were 127 × 10 × 10 mm^3. The test method is generally reproducible to an accuracy of ±0.1 %.

Vertical burning test (UL-94)

The vertical burning test was carried out on a CFZ-2-type instrument (Jiangning Analysis Instrument Company, China) according to the UL-94 test standard. The dimensions of specimens were 130 × 13 × 3 mm^3.

Cone calorimeter

The cone calorimeter (Stanton Redcroft, UK) tests were performed according to ISO 5660 standard procedures. Each specimen of dimensions 100 × 100 × 3 mm^3 was put on a horizontal aluminum tray and exposed horizontally to an incident and external heat flux of 35 kW m^{-2}. Flame-out was defined as the extinguishment of the visible yellow flame. The value for amount of residue was taken at flame-out, which was characterized as the flaming burning before the residues were consumed in the

subsequent afterglow. In additional experiments, fire residues were removed from the cone calorimeter at flame-out and quenched with liquid nitrogen in order to avoid thermooxidation of the subsequent after glow and thus to observe the residue structures formed during combustion. Time to ignition (TTI), total heat release (THR), peak of heat released rate (p-HRR), and amount of residue after combustion will be obtained and discussed. Results correspond to mean values obtained from two or three experiments [18, 19]. The experimental error for all mentioned parameters is ±10 %.

Results and discussions

Flame retardancy

As shown in Table 1, the flame-retardant properties of PP composites were conducted by LOI and UL-94 tests. As we know, LOI and UL-94 tests are the basic and intuitive methods to detect the flame retardancy of materials. Apparently, the LOI value of pure PP is only 17.0 % and cannot obtain any levels in UL-94 tests. This fact demonstrates the flammability and severe melt dripping of pure PP materials. This seriously restricts the further application in more fields. As for PP/MPP, PP/DPER, and PP/EG, the LOI values of these samples are 24.5, 21.0, and 25.5 %, respectively. Even though the flame retardancy of these systems is enhanced in a small scale, none of these samples can pass the UL-94 tests. That is to say, the flame retardance of PP materials cannot be effectively improved by compositing with acid source or char agent alone. For PP/MPP/DPER system, the LOI values of PP composites are much higher than that of PP binary system. With the ratio of MPP/DPER on, the LOI values of PP/MPP/DPER system first increase then decrease and all of them can obtain a rating in the UL-94 tests (3.2 mm). The main reason may be originated from the synergistic effect between MPP and DPER in flame-retarding PP materials, which will be discussed as follows. Among these, PP/MPP/DPER 3/1 achieves the maximum value in LOI tests and acquires V-0 (3.2 mm) and V-1 (1.6 mm) rating in UL-94 tests. Thus, we regard the optimum ratio of MPP/DPER at 3/1 in PP composites. To simplify, the MPP/DPER (3/1) system is named intumescent flame retardant (IFR) in this article.

Moreover, the effect of EG on the flame-retardant properties of PP/MPP/DPER system was systematically investigated. In these samples, the ratio of MPP/DPER keeps at 3/1 and the content of flame retardants in matrix is 30 phr per 100 phr PP. As shown in Table 1, the LOI values of PP/MPP/DPER/EG system first increase then slightly decrease with the increment content of EG and all samples can pass the UL-94 tests (3.2 and 1.6 mm). On one hand, the intumescent char layer is composed of the thermal esterification reaction between MPP and DPER when the content of EG is low. However, the quality and structure of char layer is not very hard and dense that cannot effectively act as a barrier to restrain the heat and mass transfer process; on the other hand, the balance for the synergistic effect between MPP/DPER and EG tends to be optimal that leads to the increase in flame retardancy. In this condition, the flame-retardant properties of PP/IFR/EG composite first increase with the increment loading of EG. When the content of EG further increases, the excess EG will cause a slight decrease in flame retardancy due to its random expansion process. This may lead to the decrease in flame retardancy with the further increase in percentage of EG. Except that, EG possesses the better flame-retardant effect than MPP/DPER when they are in the same IFR/EG system. Therefore, LOI value and vertical burning test rating of PP/IFR/EG composite first increase then decrease little with the increase amount of EG. Besides, the optimal synergistic effect for PP composites was found in the loadings of 10.0 wt% EG in PP composites that possess 33.2 % LOI value and V-0 ratings in UL-94 tests. The detailed flame-retardant mechanism will be detailedly depicted in next section.

Cone calorimeter tests

As we know, cone calorimeter tests are an effective approach to evaluate the combustion behavior of flame-retarding polymeric materials. It is useful for the small-scale assessment of several reactions of fire parameters, and this method is widely employed for the development of new materials. Thus, cone calorimeter tests were adopted in investigating the combustion behavior of PP composites. The heat release rate (HRR), total heat release (THR), mass loss rate (MLR), and smoke production rate (SPR) curves of PP composites are shown in Figs. 1, 2, 3, and 4. And the detailed data obtained from cone calorimeter

tests are recorded in Table 2. In Fig. 1, it can be observed that neat PP burns very fast after ignition with a p-HRR value of 1165.5 kW/m^2 with the TTI value of 38 s, which demonstrates the flammability of PP. The p-HRR value of PP/MPP/DPER 3/1 decreases to 427.6 kW/m^2, which illustrates that MPP/DPER system can greatly reduce the p-HRR value of PP materials. Besides, the TTI value of PP/MPP/DPER 3/1 appears at 45 s due to the improvement in thermal stability of PP composites. Surprisingly, the incorporation of EG into PP/IFR system can further lower the p-HRR value and TTI value of PP composites. Except that, it can be observed that the HRR curves of PP/MPP/DPER and PP/IFR/EG show two peaks in Fig. 1. The first HRR peak for PP/MPP/DPER is assigned to the gradual formation of the swollen protective char layer by the interaction between flame-retardant particles (MPP and DPER). After the first HRR peak, the second HRR peak appears an increase for PP/MPP/DPER, in which the increment in HRR value is not restrained and suppressed due to the presence of the ineffective protective char layer on the surface of PP composites during combustion [20, 21]. Compared with PP/MPP/DPER, the second HRR curve of PP/MPP/DPER/EG system nearly presents a plateau with low HRR value which indicates that the efficient protective char layer gradually forms as PP composites are continuously exposed to the fire. In the condition, the "barrier effect" of protective char layer for PP/MPP/DPER/EG during the thermal degradation can lead to the improvement in flame retardancy [22]. Except

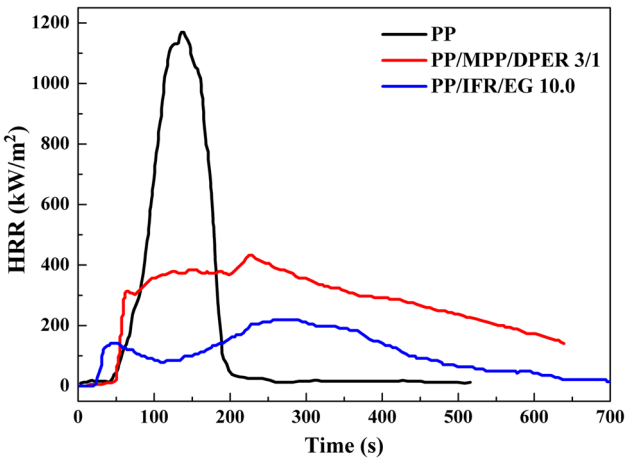

Figure 1 HRR curves of PP composites.

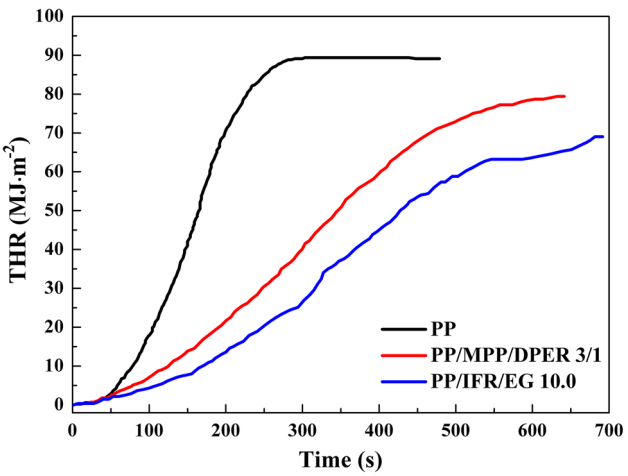

Figure 2 THR curves of PP composites.

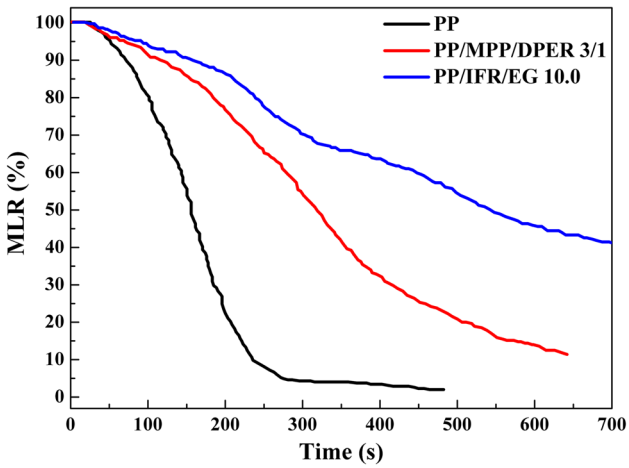

Figure 3 MLR curves of PP composites.

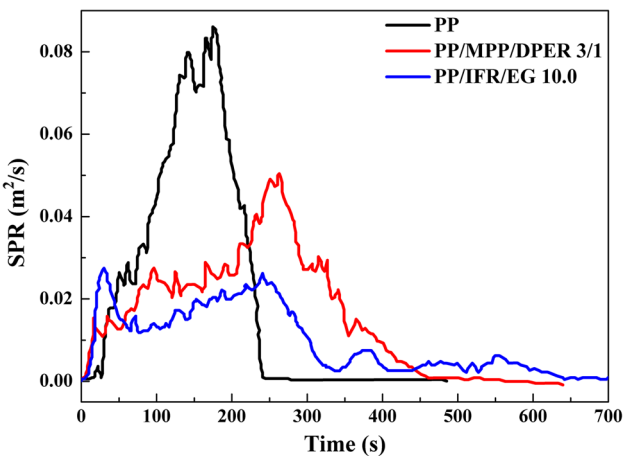

Figure 4 SPR curves of PP composites.

Table 2 Cone calorimeter data of PP composites

Sample	TTI (s)	p-HRR (kW/m^2)	Time to p-HRR (s)	FGR (kW/m^2)	THR MJ/m^2	p-SPR (m^2/s)	AEHC (MJ/kg)
PP	38	1165.5	137.6	8.47	89.1	0.085	39.35
PP/MPP/DPER 3/1	45	427.6	226.6	1.89	79.4	0.051	39.21
PP/IFR/EG 10.0	20	218.2	272.9	0.80	68.7	0.027	39.57

that, THR value of PP/MPP/DPER/EG is much lower than that of PP and PP/MPP/DPER due to the synergistic effect of EG and IFR in suppressing the heat production rate of PP matrix in Fig. 2. In this condition, the mass loss rate of PP composites is remarkably restrained for MPP/DPER and MPP/DPER/EG system as shown in Fig. 3. The latter can further enhance the mass residue of PP materials due to the introduction of EG that is ascribed to the synergistic char-forming mechanism between IFR and EG. And the detailed process will be depicted in the next section. Based on the HRR curves, fire growth rate (FGR) has been calculated to assess the fire hazard of the composite according to the following equation [23, 24].

$$\mathrm{FGR} = \mathrm{p-HRR/Time\ to\ p-HRR}.$$

Generally, a lower FGR value indicates that the time to flashover is delayed [25]. As shown in Table 2, the lowest FGR value appears in PP/MPP/DPER/EG system, demonstrating that the introduction of EG can drastically reduce the FGR value of PP and PP composite. Consequently, it can effectively prolong the time to escape in a real accident. Moreover, it is clear that MPP/DPER can decrease the p-SPR value of PP matrix from 0.085 to 0.051 m^2/s as shown in Fig. 4. Besides, the MPP/DPER/EG system can further reduce the p-SPR value due to the synergism effect between MPP/DPER and EG in flame-retarding PP materials. Furthermore, the average effective heat of combustion (AEHC) values of PP, PP/MPP/DPER, and PP/IFR/EG was also investigated by cone calorimeter tests. It can be observed that the AEHC values of these samples are nearly similar. This illustrates that IFR and EG in PP matrix experience a condensed flame-retardant mechanism [26].

In conclusion, the flame-retardant properties of PP composites was greatly improved by the incorporation of MPP/DPER and EG. Moreover, the synergism effect between MPP/DPER and EG can greatly reduce the HRR, THR, FGR, MLR, and SPR value that indicates the combustion of PP matrix is drastically suppressed in the real fire. Thus, the LOI value of PP composites is raised in large extent and it can reach a V-0 rating in UL-94 tests.

Thermal behavior of MPP, DPER, EG, and their mixture

The thermal behavior of MPP, DPER, EG, and their mixture was also investigated by TGA tests, as shown in Fig. 5a. Besides, the differential thermal gravity (DTG) of these samples was also investigated, as shown in Fig. 5b. In DTG curve, MP undergoes three thermal decomposition steps, which are 260–340, 340–450, and 450–700 °C, respectively. Based on the investigation of Costa et al. [27], the first two steps correspond to the conversion of MPP into melamine pyrophosphate and melamine phosphate. After that, the further thermal decomposition of MPP is ascribed to the thermal degradation of melamine from MPP for the release of NH_3 and H_2O. At last, the phosphorus oxides (P_2O_5 or P_4O_{10}) are formed via these procedures with 23 % weight residue at 800 °C. The thermal decomposition curve of DPER is a one-step process, which is from 250 to 450 °C. However, due to lack of acid source, the further thermal degradation of DPER leads to no residue at high temperature. Except that, in order to research the chemical interaction between MPP and DPER, the experimental and calculated TGA and DTG curves were revealed by comparison. Here, the calculated curve (cal) of a mixture of MPP and DPER shows the thermal degradation state by the linear combination of two components based on the mass percentage, which is in condition of assuming that the two components do not affect each other [28]. Compared with the calculated curve, the initial decomposition temperature of MPP/DPER system obviously decreases. Besides, the maximum decomposition rate of MPP/DPER (exp) in this process is slower than MPP/DPER (cal) in 420–540 °C, which may be attributed to thermal esterification reaction between MPP and DPER. This

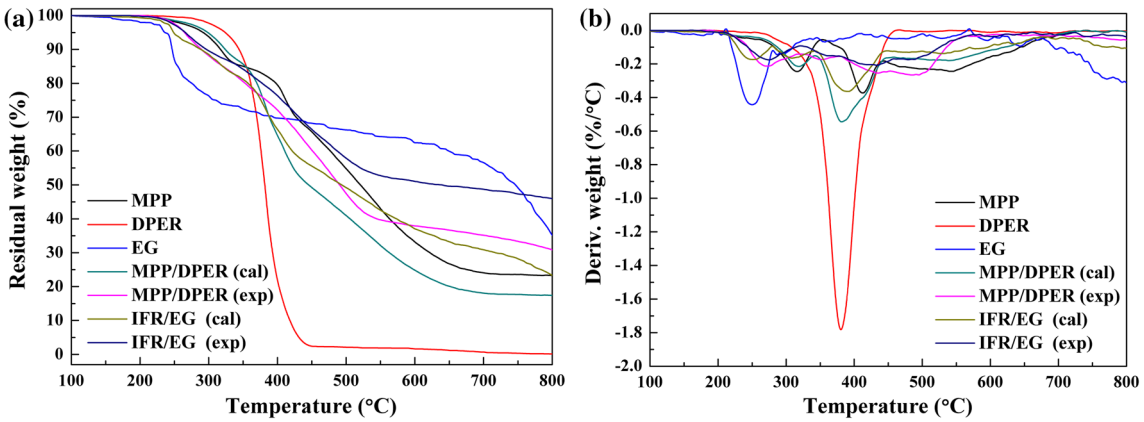

Figure 5 Thermal behavior of MPP, DPER, EG, and their mixture, **a** TGA curves, **b** DTG curves.

procedure may slow down the thermal decomposition rate of polymer composites during combustion. When the temperature is above 360 °C, the char residue of MPP/DPER (exp) exceeds MPP/DPER (cal). To our surprise, the char residue at 800 °C for MPP/DPER (exp) is 10 % higher than that of MPP/DPER (cal). Based on these facts, it can deduce that a strong chemical interaction between MPP and DPER occurs during thermal decomposition process that becomes the main reason in improving the flame retardancy of polymer composites. As shown in Fig. 5a, the thermal degradation of EG focuses on 200–300 °C, which is attributed to the expansion process of EG during heat [29]. Due to the "popcorn effect" of EG [30], the thermal stability of EG is unstable that results in the further weight loss from 600 to 800 °C, as shown in Fig. 5b. Moreover, the experimental and calculated TGA and DTG curves of MPP, DPER, and EG were revealed by comparison. Compared with the calculated curves, MPP/DPER/EG system possesses much higher char residue, demonstrating the synergistic effect between MPP/DPER and EG in char-forming process. Furthermore, the synergistic effect becomes the main reason for the improvement in flame retardancy of PP materials.

Thermal decomposition of PP composites

The thermal degradation process of PP composites in nitrogen atmosphere was systematically investigated by TGA analysis, as shown in Figs. 6a and 7a. Besides, the differential thermal gravity (DTG) of these curves was also investigated, as shown in Figs. 6b and 7b. The detailed TGA data which include the initial decomposition temperature (T_{on}, 5 % weight loss), the temperature at maximum weight loss (T_{max}), and the char residue at 500, 600, and 700 °C are listed in Table 3. The accuracy of these data is ±0.1 °C and 0.01 %, respectively. As presented in Fig. 6 and Table 3, the initial degradation temperature of pure PP is 278.9 °C. Except that, it is obviously observed that the thermal degradation of PP presents a one-step process. Unfortunately, no char residue is left for pure PP above 500 °C, illustrating the complete decomposition and inflammable property. For PP/MPP/DPER system, two weight loss peaks can be found in Fig. 6b. In order to simplify, the intumescent flame-retardant (IFR) system composed of MPP and DPER in the ratio of 3/1 is named IFR. The first weight loss peak from 260 to 350 °C is ascribed to the thermal decomposition and chemical reaction for flame retardants. The main formation process of char layer may predominantly occur at this stage, which can be further confirmed by FTIR spectra as follows. And the maximum decomposition process happens at 458.9 °C that is much higher than that of neat PP. It demonstrates that the thermal stability of PP materials is improved by introducing MPP and DPER into the system. Moreover, the residue of PP/MPP/DPER system at 500, 600, and 700 °C is 9.04, 7.42, and 6.87 %, respectively. As for PP/EG composites, the T_{on} value is obviously advanced to 259.9 °C, which is primarily attributed to the thermal expansion of EG in low-temperature zone. The T_{max} value of PP/EG is similar to that of PP, while R_{max} value of PP/EG is much lower than PP. This fact indicates that the thermal decomposition of PP composites can be slowed down but the thermal stability cannot be improved by compositing with EG alone. Even though the high residue content appears in PP/EG, the thermal stability decreases in 700–800 °C as

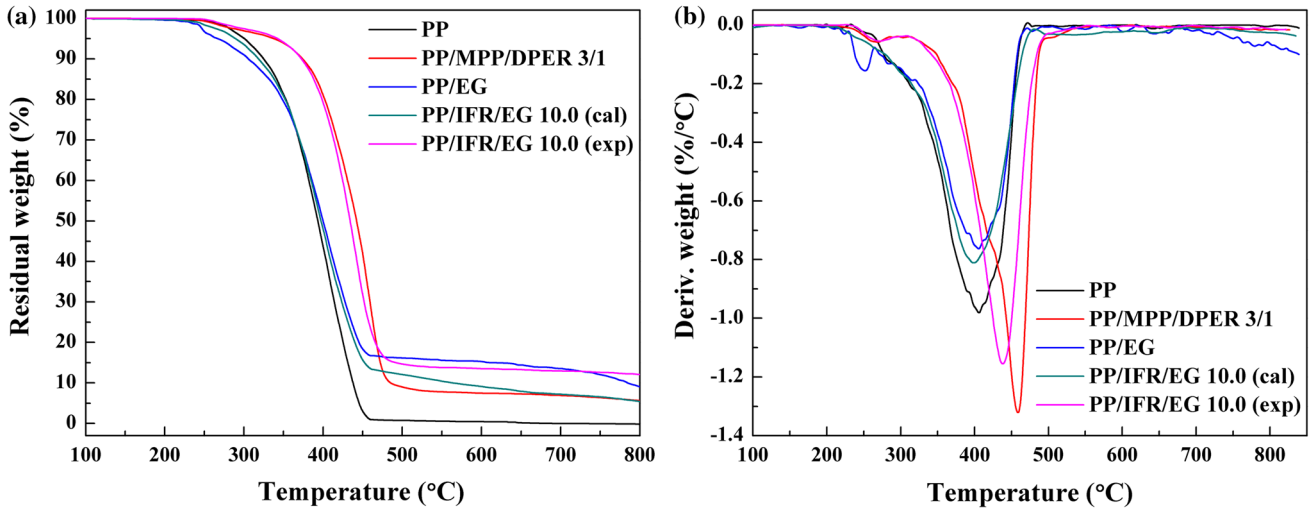

Figure 6 Thermal decomposition of PP composites, **a** TGA curves, **b** DTG curves.

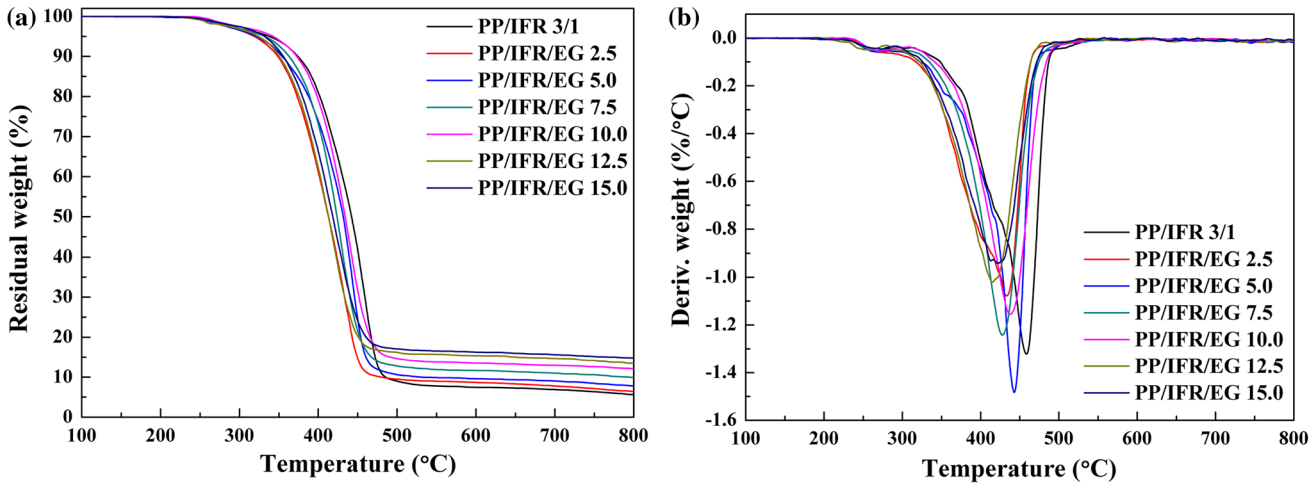

Figure 7 Effect of EG on thermal decomposition of PP composites, **a** TGA curves, **b** DTG curves.

shown in Fig. 6b. In order to certify the chemical interaction between IFR and EG in PP composites, the experimental and calculated TGA and DTG curves of PP/IFR/EG system were also carried out. Compared with PP/IFR/EG 10.0 (cal), the T_{on} and T_{max} values of PP/IFR/EG 10.0 (exp) is much higher. The reason for this fact is caused by the strong interaction between IFR and EG. On one hand, the formation of primary residue among flame retardants can improve the onset degradation process; on the other hand, the estificated reaction between MPP and DPER will accelerate the char-forming process to enhance the thermal stability of PP composites. Most of all, the char residue for PP/IFR/EG 10.0 (exp) at 500–700 °C is higher than PP/IFR/EG 10.0 (cal) that can further explain the effective reaction between IFR and EG in enhancing char-forming ability of PP composites. Based on these facts, the synergistic effect between IFR and EG found in the LOI and UL-94 tests can be further confirmed.

Furthermore, the effect of EG loadings on the thermal behavior of PP/IFR/EG composites was also investigated by TGA tests, as presented in Fig. 7. In evidence, the char residue of PP composites above 600 °C gradually increases with the increment content of EG. However, as shown in Fig. 7b, the T_{max} value of PP composites greatly decreases when the

Table 3 TGA data of PP composites in nitrogen atmosphere

Sample code	T_{on}^{a}	T_{max}^{b}	Char residues (wt%)			R_{max}^{c}
	(°C)	(°C)	500 °C	600 °C	700 °C	(%/ °C)
PP	300.1	406.8	0	0	0	−0.96
PP/MPP/DPER 3/1	338.8	458.9	9.04	7.42	6.87	−1.33
PP/EG	259.9	402.6	16.14	15.28	13.55	−0.76
PP/IFR/EG 10.0 (cal)	290.5	398.2	11.75	8.58	7.42	−0.81
PP/IFR/EG 10.0 (exp)	341.8	438.3	13.09	11.93	11.35	−1.16

[a] T_{on}: the temperature at 5 % weight loss

[b] T_{max}: the temperature at maximum weight loss rate

[c] R_{max}: maximum decomposition rate

content of EG is above 10 %. The decrease in thermal stability is mainly caused by the excess EG. And the optical photos indicate that the undirectional expansion of EG during combustion will weaken the density of char residue on the surface of PP composites. Combined with the results of LOI and UL-94 tests, it demonstrates that the optimum loading of EG is 10 % in PP composites in view of flame retardancy and char residue content.

FTIR spectra of residue for MPP/DPER/EG at different temperatures

In order to study the chemical interaction of MPP/DPER/EG system during the thermal oxidative degradation, the char residue obtained at different thermal pyrolysis temperatures was detected by FTIR spectra. The mixture of MPP/DPER/EG was heated at 10 °C/min heating rate in a muffle furnace during air atmosphere [31]. The residues were obtained by heating the mixture powder to 300, 350, 400, 450, 500, and 600 °C in air and maintained 10 min at every temperature, respectively. The detailed FTIR curves of these residues are shown in Fig. 8. Due to the little absorption peaks for EG, FTIR spectra of mixture at 25 °C are mainly composed of the characteristic absorption of MPP and DPER. The peaks at 3100–3400 cm^{-1} belong to $–NH_2$ and –OH groups, respectively. The absorption of –CH– or $–CH_2–$ groups on the structure of DPER appears in 2945 and 2886 cm^{-1}. Besides, the peaks at 1671, 1512, and 1329 cm^{-1} are assigned to the –C=N– groups from s-triazine ring on MPP. Except that, the peaks at 1283, 1167, 1093, and 871 cm^{-1} are attributed to the structure of P=O, C–O–C, and P–O–P groups, which are originated from MPP and DPER. When the system was heated to 300 °C, it can be obviously found that the two peaks at 1060 and 883 cm^{-1} appear in FTIR spectra. It is ascribed to the characteristic vibration of P–O–P groups that demonstrate the thermal hydration of MPP to the conversion of MPP into melamine pyrophosphate or melamine phosphate. At 350 °C, the FTIR spectra of char residue keep nearly unchanged. As for 400 °C, the difference from 300 and 350 °C is focused on the appearance of 1642 cm^{-1}, which is mainly due to the unsaturated –C=C– structure generating from the thermal degradation of DPER. And the main changes are that the peaks for P–O–P at 1060 and 883 cm^{-1} shift to 1087 and 879 cm^{-1}, respectively. As we know, the two peaks are ascribed to the absorption of P-O bonds in P–O–C groups. Thus, it can be concluded that the cross-linking reaction between MPP and DPER occurs. Simultaneously, the peaks of –OH and $–NH_2$ groups gradually disappear during 350–400 °C that

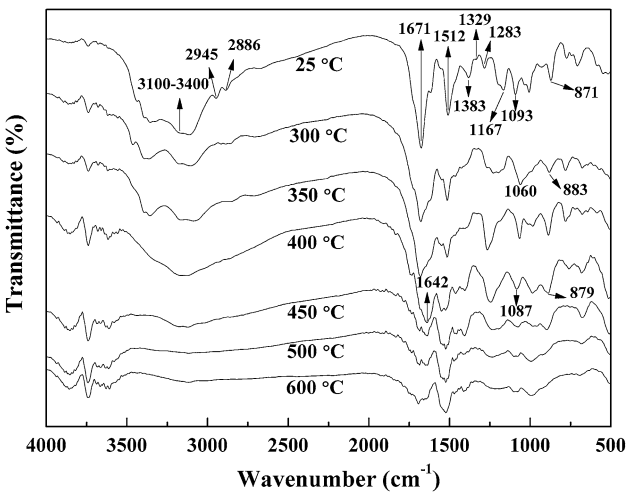

Figure 8 FTIR spectra of char residue for MPP/DPER/EG system at different temperatures.

converts to the gases (NH_3 and H_2O). Due to this process, the compact and dense condensed char layer was constituted by the cross-linking structure and further the intumescent char layer can be formed by these gases release in the inner char residue above PP composites. After that, the chemical structure of system nearly changes less with the increment of pyrolysis temperature. Therefore, the main char-forming process of flame retardants happens at 350–400 °C and the potential flame-retardant mechanism can be achieved.

Char residue analysis

To research the surface morphology and chemical structure of the char residue after burning, PP/IFR/EG samples with different weight ratios were heated in the muffle furnace at 600 °C for 15 min. As shown in Fig. 9, the surface morphology of char residue of PP composites was investigated by optical photos. The char residues were obtained by heating these samples in the muffle furnace at 600 °C for 15 min, which can make the complete combustion of PP composites. Obviously, it can be observed that nearly no char residue was left after combustion that intuitively illustrates the flammability of pure PP. Even if the char layer was formed for PP/MPP/DPER system, the degree of expansion for this system cannot further improve the flame-retardant properties of PP. Thus, we combine IFR and EG to construct a novel flame-retardant system in this article in order to promote the high-quality char layer during combustion. As shown in Fig. 9c, the obvious collapse structure for char residue was observed when the loadings of EG is low. With the increment content of EG in flame-retardant system, the morphology of char residue tends to be continuous, dense, and intumescent as shown in Fig. 9d–f that is mainly attributed by the synergistic effect between IFR and EG in the char-forming process of PP composites after combustion. However, the surface of char layer presents cellular and less compact when the content of EG exceeds 10 %. This is mainly ascribed to the "popcorn effect" during combustion that is originated to the random expansion of EG. In this condition, the flame-retardant properties of PP composites are weakened which are consistent with the results of LOI and UL-94 tests. Based on these facts, the results

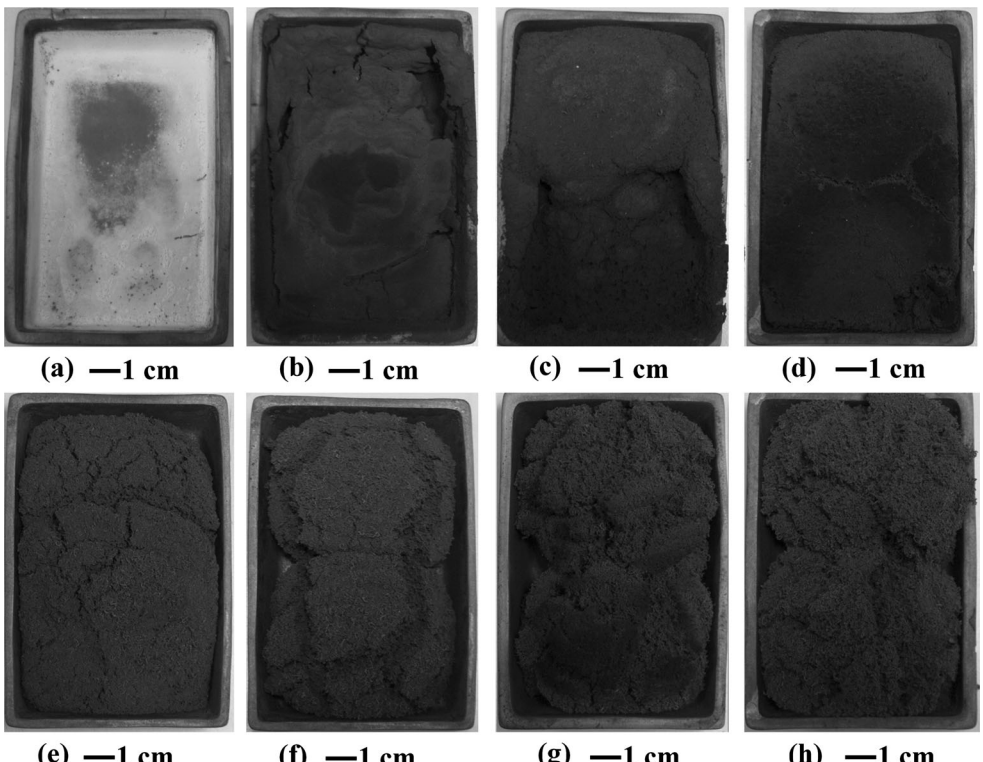

Figure 9 Optical photos of char residue for PP composites after combustion, **a** PP, **b** PP/MPP/DPER 3/1, **c** PP/IFR/EG 2.5, **d** PP/IFR/EG 5.0, **e** PP/IFR/EG 7.5, **f** PP/IFR/EG 10.0, **g** PP/IFR/EG 12.5, **h** PP/IFR/EG 15.0.

can also explain the synergistic effect of IFR and EG in improving the flame-retardant properties of PP composites.

Furthermore, the chemical structure of char residue for PP/MPP/DPER/EG system after combustion was also investigated by FTIR spectra. As shown in Fig. 10, the absorption peak at 3453 cm^{-1} is assigned to $–NH_2$ groups. And the peak at 1642 cm^{-1} is mainly due to the –C=C– groups, which is originated to the formation of "graphite-like" structure after combustion for PP composites. The "graphite-like" structure can be confirmed by Raman analysis in Supporting Information. The characterized peaks at 1743, 1547, 1515, and 1402 cm^{-1} are ascribed to –C=O, –NH–, and –C=N– groups in s-triazine ring, respectively. These facts can further indicate the formation of oxidized groups for PP composites during combustion. Most of all, the peaks appearing at 1087 and 879 cm^{-1} are mainly attributed to the symmetric stretching of P–O bonds in the structure of P–O–C groups [32]. Therefore, FTIR spectra conform the formation of P–O–C bonds in char layer, which demonstrates the chemical cross-linking reaction between MPP and DPER. Based on abovementioned analysis, the formation of cross-linked structure will play a significant role in char residue after the combustion of PP composites. Along with the effect of EG, they can effectively promote to form the compact and swell "graphite-like" char layer in the surface of residue (Fig. 9) and improve the flame-retardant properties of PP materials by compositing with this novel flame-retardant system.

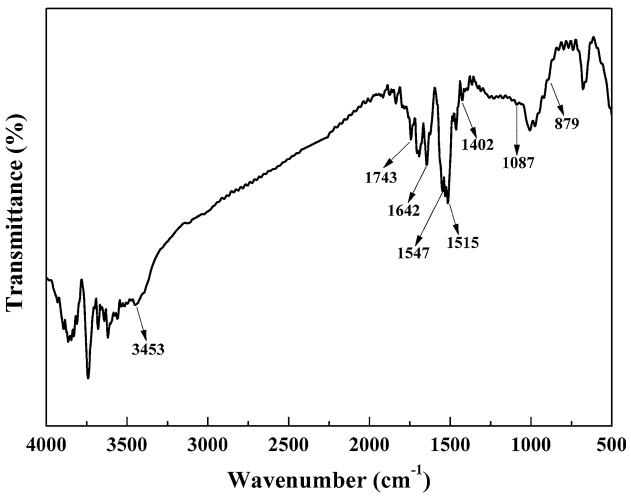

Figure 10 FTIR spectra of char residue of PP/IFR/EG 10.0 after combustion.

XPS spectra of residue of PP/IFR/EG system

As we know, X-ray photoelectron spectroscopy (XPS) can provide further information about elemental composition and the elemental content of char residue in detail, which supplements the results from FTIR spectra. The XPS spectra of C_{1s}, O_{1s}, N_{1s} and P_{2p} of char residue from PP/IFR/EG system after the combustion tests are shown in Fig. 11a–d. Besides, the detailed assignations of these peaks are systematically recorded in Table 4. As shown in Fig. 11a, the two peaks for C_{1s} spectra are observed with the binding energy at 284.8 and 286.1 eV, respectively. They can be assigned to C–C or C=C bonds in aliphatic, aromatic structures and graphite and the C–O bonds in the P–O–C groups in ether and phosphate, which is well consistent with the results of FTIR spectra above. Moreover, the spectra of O_{1s} of char residue present two bands at 531.5 and 533.0 eV as shown in Fig. 11b that can be assigned to the –O– and =O– groups, respectively. The two bands are mainly contributed by –P=O or –C=O groups in phosphate and carbonyl compounds and the –O– bond in C–O–C, O=P–O–C, and O=C–O–P from the aromatic compounds of residual char, respectively [33, 34]. And the band at 533 eV is ascribed to P–O bonds in the P–O–C groups that can be proved by FTIR spectra as shown in Fig. 10. In Fig. 11c, the XPS spectra of N_{1s} exhibit a peak with binding energy at 399.5 eV, which can be assigned to the quaternary nitrogen in NH_4^+ groups. As for P_{2p}, a band is found with binding energy at 134.5 eV as shown in Fig. 11d [35], which can be assigned to the P–O in P–O–C groups. This can further verify the esterification reaction between MPP and DPER during thermal decomposition of PP composites. And this chemical structure can enhance the thermal stability and integrity of char residue for PP composites.

Potential flame-retardant mechanism

Based on the abovementioned results, the potential flame-retardant mechanism of MPP/DPER/EG in PP matrix has been primarily proposed, as shown in Scheme 1. First, the hydration of MPP at 300–350 °C during thermal flow can lead to the formation of melamine pyrophosphate or melamine phosphate. After that, the further chemical cross-linking reaction between MPP and DPER results in the formation of esterifiable structure with P–O–C groups in

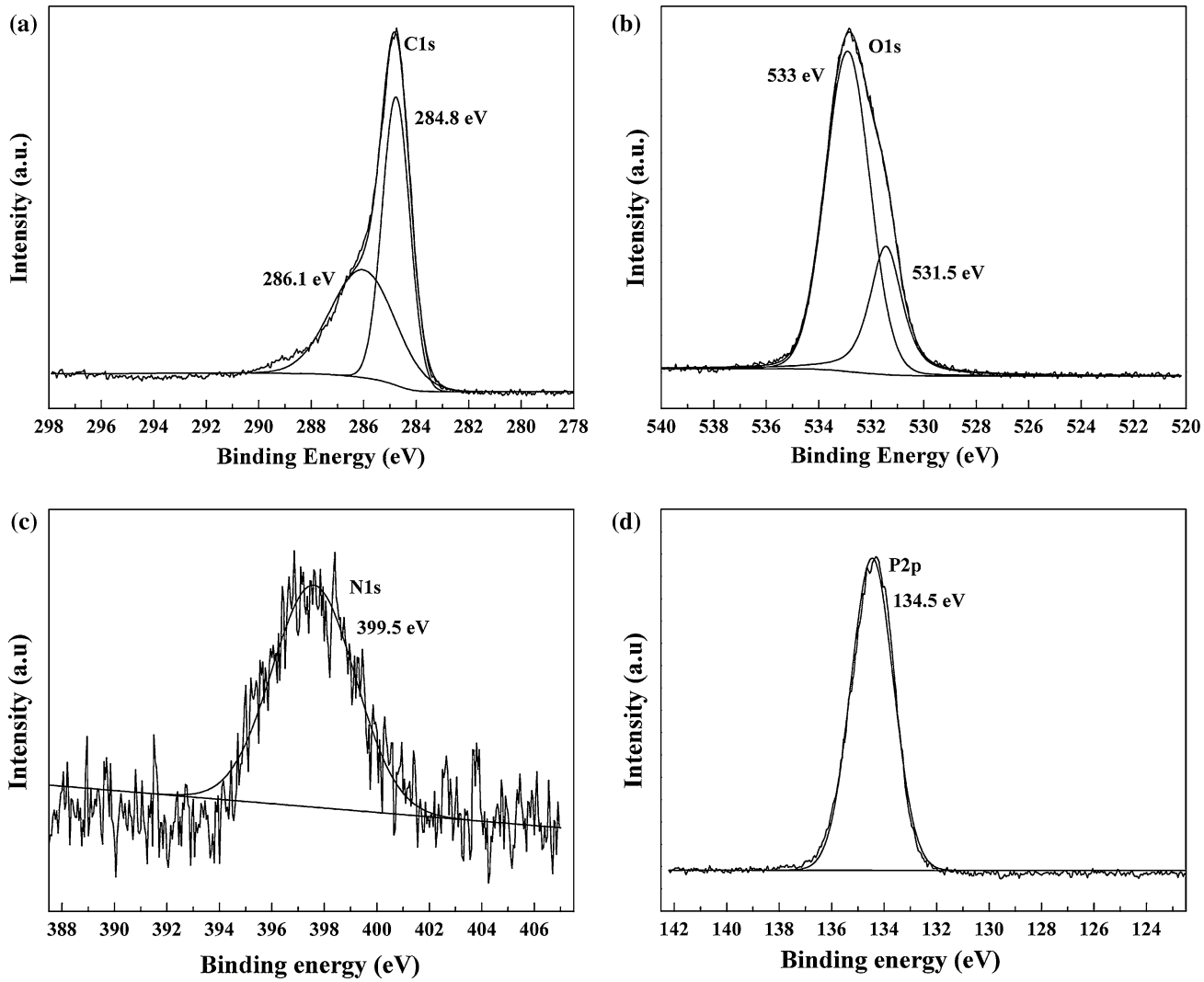

Figure 11 XPS spectra of char residue from PP/IFR/EG 10.0 after combustion, **a** C_{1s} peaks, **b** O_{1s} peaks, **c** N_{1s} peaks, **d** P_{2p} peaks.

350–400 °C, which can be affirmed in FTIR and XPS spectra. By this process, the compact and dense char layer on the surface of PP composites is elementarily formed in the solid phase, as shown in Fig. 9c. Simultaneously, the inert gases release (NH_3 and H_2O) during this procedure from MPP can promote char residue to expand to some extent. Along with the swell effect of EG, the high-quality char residue system is further generated that possesses dense and compact char layer on the surface and intumescent, thick and porous "foam-like" structure inside the composites, as shown in Fig. 9e. This char residue acting as a barrier can effectively limit the mass and heat transfer between gas phase and condensed phase and protect the underlying substrate from further thermal decomposition during combustion. Based on these facts, the flame-retardant properties of PP composites are greatly improved. As we know, this system undergoes the classic condensed flame-retardant mechanism during thermal degradation.

Table 4 Identification of functional groups for PP/IFR/EG composites after combustion

Element	Binding energy (eV)	Group
C_{1s}	284.8	C–C or C=C
	286.1	C–O and C–O–P
O_{1s}	531.5	–O– group
	533	=O– group
N_{1s}	399.5	NH_4^+
P_{2p}	134.5	P–O–C

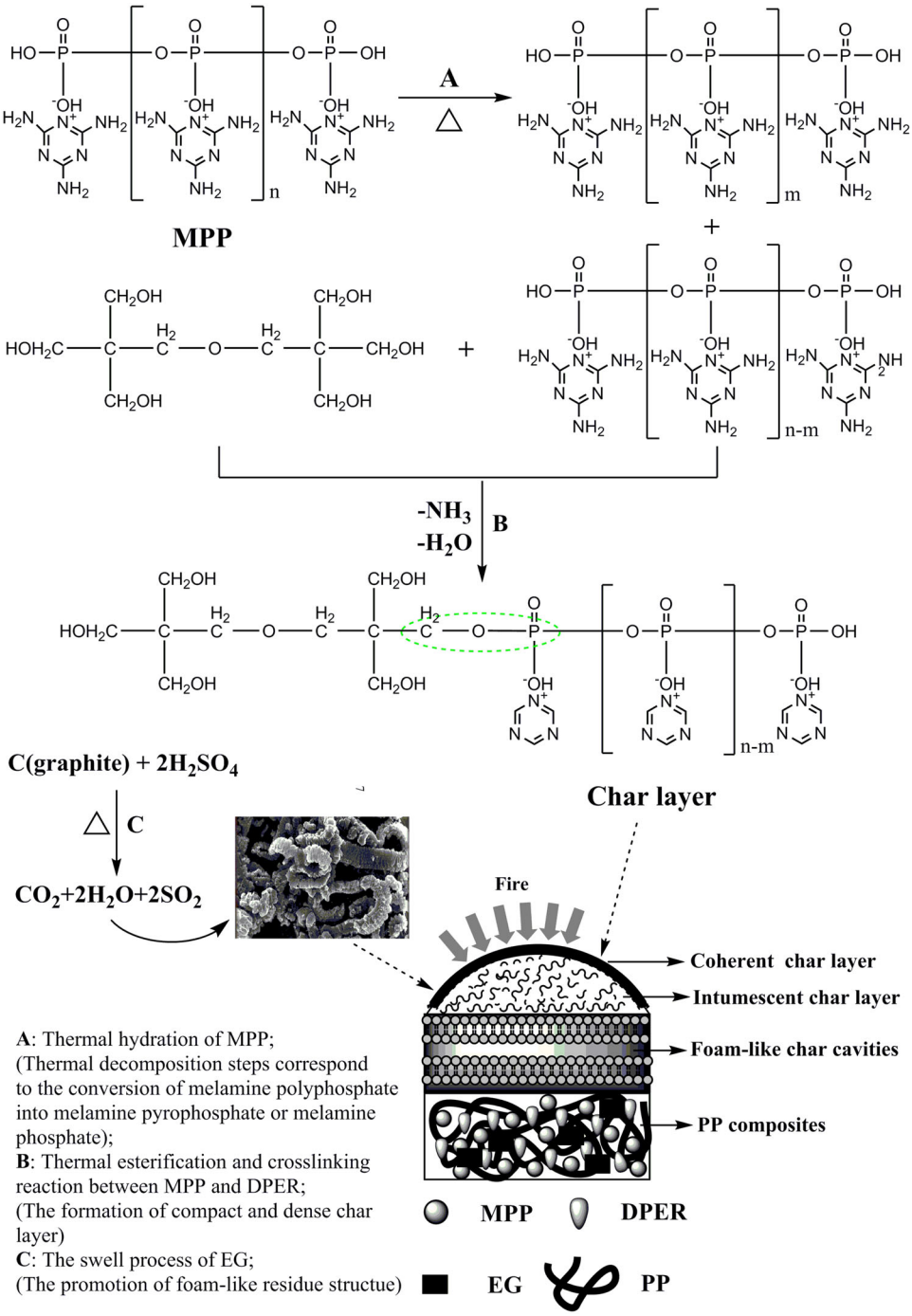

Scheme 1 The possible flame-retardant mechanism of IFR and EG in PP composites.

Conclusion

In this paper, the synergistic effect between IFR and EG in flame-retarding PP materials was systematically investigated. LOI and UL-94 tests demonstrate that the incorporation of EG into the PP/IFR system can greatly improve the flame-retardant properties of PP materials. The results confirm that the synergistic effect for the IFR/EG system exists in improving the flame-retardant properties of PP. And FTIR spectra of residue for MPP/DPER/EG system obtained at different temperatures indicate that the main char-

formation process of MPP/DPER/EG system occurs at 350–400 °C. The thermal decomposition and thermal oxidation were employed in investigating the thermal behavior of PP composites, which can further illustrate the synergistic effect between IFR and EG in promoting the char-forming process of PP composites. Moreover, the char residue for PP composites after combustion was systematically analyzed by FTIR and XPS spectra. Based on the analysis, a potential condensed flame-retardant mechanism was primarily proposed.

Acknowledgements

This work was supported by the National Natural Science Foundation of China (Nos. 51275555, 51325501 and 5147200) and Science and Technology Development Project of Jilin Province (No. 20150519007JH).

Electronic supplementary material: The online version of this article (doi:10.1007/s10853-016-9887-6) contains supplementary material, which is available to authorized users.

References

[1] Gonzalez-Calderon JA, Vallejo-Montesinos J, Mata-Padilla JM, Pérez E, Almendarez-Camarillo A (2015) Effective method for the synthesis of pimelic acid/TiO_2 nanoparticles with a high capacity to nucleate β-crystals in isotactic polypropylene nanocomposites. J Mater Sci 50:7998–8006. doi:10.1007/s10853-015-9365-6

[2] Subasinghe ADL, Das R, Bhattacharyya D (2015) Parametric analysis of flammability performance of polypropylene/kenaf composites. J Mater Sci 1:1–11. doi:10.1007/s10853-015-9520-0

[3] Chen SH, Wang XD, Ma XQ, Wang KS (2015) Morphology and properties of polypropylene/nano-$CaCO_3$ composites prepared by supercritical carbon dioxide-assisted extrusion. J Mater Sci 1:1–11. doi:10.1007/s10853-015-9272-x

[4] Qian XD, Song L, He YB, Yu B, Shi YQ, Hu Y, Yuen RKK (2014) Organic/inorganic flame retardants containing phosphorus, nitrogen and silicon: preparation and their performance on the flame retardancy of epoxy resins as a novel intumescent flame retardant system. Mater Chem Phys 143:1243–1252

[5] Wang J, Cai XF (2012) Synergistic effect of a novel charring agent with ammonium polyphosphate on flame retardancy and thermal degradation of acrylonitrile-butadiene-styrene copolymer. Polym Int 61:703–710

[6] Zhang Y, Chen XL, Fang ZP (2013) Synergistic effects of expandable graphite and ammonium polyphosphate with a new carbon source derived from biomass in flame retardant ABS. J Appl Polym Sci 128:2424–2432

[7] Quédé A, Cardoso J, Le Bras M, Delobel R, Goudmand P, Dessaux O, Jama C (2002) Thermal stability and flammability studies of coated polymer powders using a plasma fluidized bed process. J Mater Sci 37:1395–1399. doi:10.1023/A:1014576730732

[8] Le Bras M, Bourbigot S, Revel B (1999) Comprehensive study of the degradation of an intumescent EVA-based material during combustion. J Mater Sci 34:5777–5782. doi:10.1023/A:1004758218104

[9] Camino G, Costa L, Trossarelli L (1984) Study of the mechanism of intumescence in fire retardant polymers: part I-Thermal degradation of ammonium polyphosphate-pentaerythritol mixtures. Polym Degrad Stab 6:243–252

[10] Camino G, Costa L, Trossarelli L (1984) Study of the mechanism of intumescence in fire retardant polymers: part II-Mechanism of action in polypropylene-ammonium polyphosphate-pentaerythritol mixtures. Polym Degrad Stab 7:25–31

[11] Camino G, Costa L, Trossarelli L (1984) Study of the mechanism of intumescence in fire retardant polymers: part III-Effect of urea on the ammonium polyphosphate-pentaerythritol system. Polym Degrad Stab 7:221–229

[12] Camino G, Costa L, Trossarelli L, Costanzi F, Landoni G (1984) Study of the mechanism of intumescence in fire retardant polymers: part IV-Evidence of ester formation in ammonium polyphosphate-pentaerythritol mixtures. Polym Degrad Stab 8:13–22

[13] Camino G, Costa L, Trossarelli L (1985) Study of the mechanism of intumescence in fire retardant polymers: part V-Mechanism of formation of gaseous products in the thermal degradation of ammonium polyphosphate. Polym Degrad Stab 12:203–211

[14] Camino G, Costa L, Trossarelli L, Costanzi F, Pagliari A (1985) Study of the mechanism of intumescence in fire retardant polymers: part VI-Mechanism of ester formation in ammonium polyphosphate-pentaerythritol mixtures. Polym Degrad Stab 12:213–228

[15] Chung DDL (2016) A review of exfoliated graphite. J Mater Sci 51:554–568. doi:10.1007/s10853-015-9284-6

[16] Guan GQ, Lu JS, Jiang HL (2015) Preparation, characterization, and physical properties of graphene nanosheets and

films obtained from low-temperature expandable graphite. J Mater Sci 1:1–11. doi:10.1007/s10853-015-9422-1

[17] Vannier A, Duquesne S, Bourbigot S, Castrovinci A, Camino G, Delobel R (2008) The use of POSS as synergist in intumescent recycled poly(ethylene terephthalate). Polym Degrad Stab 93:818–826

[18] Yuan BH, Sheng HB, Mu XW, Song L, Tai QL, Shi YQ, Liew KM, Hu Y (2015) Enhanced flame retardancy of polypropylene by melamine-modified graphene oxide. J Mater Sci 50:5389–5401. doi:10.1007/s10853-015-9083-0

[19] Haile M, Fomete S, Lopez ID, Grunlan JC (2016) Aluminum hydroxide multilayer assembly capable of extinguishing flame on polyurethane foam. J Mater Sci 51:375–381. doi:10.1007/s10853-015-9258-8

[20] Zheng ZH, Sun HM, Li WJ, Zhong SL, Yan JT, Cui XJ, Wang HY (2014) Co-microencapsulation of ammonium polyphosphate and aluminum hydroxide in halogen-free and intumescent flame retarding polypropylene. Polym Compos 35:715–729

[21] Zheng ZH, Qiang LH, Yang T, Wang BN, Cui XJ, Wang HY (2014) Preparation of microencapsulated ammonium polyphosphate with carbon source- and blowing agent-containing shell and its flame retardance in polypropylene. J Polym Res 21:443–457

[22] Sengupta R, Bhattacharya M, Bandyopadhyay S, Bhowmick AK (2011) A review on the mechanical and electrical properties of graphite and modified graphite reinforced polymer composites. Prog Polym Sci 36:638–670

[23] Wang L, Yang W, Wang BB, Wu Y, Hu Y, Song L, Yuen RKK (2012) The impact of metal oxides on the combustion behavior of ethylene–vinyl acetate coploymers containing an intumescent flame retardant. Ind Eng Chem Res 51:7884–7890

[24] Wang BB, Tang QB, Hong NN, Song L, Wang L, Shi YQ, Hu Y (2011) Effect of cellulose acetate butyrate microencapsulated ammonium polyphosphate on the flame retardancy, mechanical, electrical, and thermal properties of intumescent flame-retardant ethylene–vinyl acetate copolymer/microencapsulated ammonium polyphosphate/polyamide-6 blends. ACS Appl Mater Interfaces 3:3754–3761

[25] Lu SY, Hamerton I (2002) Recent developments in the chemistry of halogen-free flame retardant polymers. Prog Polym Sci 27:1661–1712

[26] Zheng ZH, Liu SF, Wang BN, Yang T, Cui XJ, Wang HY (2015) Preparation of a novel phosphorus-and nitrogen-containing flame retardant and its synergistic effect in the intumescent flame-retarding polypropylene system. Polym Compos 36:1606–1619

[27] Costa L, Camino G, Cortemiglia MPL (1991) Overview of fire retardant mechanisms. Polym Degrad Stabil 33:131–154

[28] Tian NN, Wen X, Jiang ZW, Gong J, Wang YH, Xue J, Tang T (2013) Synergistic effect between a novel char forming agent and ammonium polyphosphate on flame retardancy and thermal properties of polypropylene. Ind Eng Chem Res 52:10905–10915

[29] Zheng ZH, Yan JT, Sun HM, Cheng ZQ, Li WJ, Wang HY, Cui XJ (2014) Preparation and characterization of microencapsulated ammonium polyphosphate and its synergistic flame-retarded polyurethane rigid foams with expandable graphite. Polym Int 63:84–92

[30] Lee S, Cho D, Drzal LT (2005) Real-time observation of the expansion behavior of intercalated graphite flake. J Mater Sci 40:231–234. doi:10.1007/s10853-005-5715-0

[31] Jiang WZ, Hao JW, Han ZD (2012) Study on the thermal degradation of mixtures of ammonium polyphosphate and a novel caged bicyclic phosphate and their flame retardant effect in polypropylene. Polym Degrad Stab 97:632–637

[32] Li J, Ke CH, Xu L, Wang YZ (2012) Synergistic effect between a hyperbranched charring agent and ammonium polyphosphate on the intumescent flame retardance of acrylonitrile-butadiene-styrene polymer. Polym Degrad Stab 97:1107–1113

[33] Dittrich B, Wartig KA, Hofmann D, Mulhaupt R, Schartel B (2013) Flame retardancy through carbon nanomaterials: carbon black, multiwall nanotubes, expanded graphite, multi-layer graphene and graphene in polypropylene. Polym Degrad Stab 98:1495–1505

[34] Liu Y, Zhao J, Deng CL, Chen L, Wang DY, Wang YZ (2011) Flame-retardant effect of sepiolite on an intumescent flame-retardant polypropylene system. Ind Eng Chem Res 50:2047–2054

[35] Wang ZY, Han EH, Ke W (2005) Influence of nano-LDHs on char formation and fire-resistant properties of flame-retardant coating. Prog Org Coat 53:29–37